Supporting Information

Synthesis, Structure and Magnetic Properties of a New Family of Tetra-nuclear $\{Mn_2^{III}Ln_2\}$(Ln = Dy, Gd, Tb, Ho) Clusters With an *Arch-Type* Topology: Single-Molecule Magnetism Behavior in the Dysprosium and Terbium Analogues.

Vadapalli Chandrasekhar,[a,b] *Prasenjit Bag,*[a] *Manfred Speldrich,*[c] *Jan van Leusen*[c] *and Paul Kögerler**[c]

[a]Department of Chemistry, Indian Institute of Technology Kanpur, Kanpur-208016, India; [b]Tata Institute of Fundamental Research, Centre for Interdisciplinary Sciences, 21 Brundavan Colony, Narsingi, Hyderabad-500075, India;

[c]Institut für Anorganische Chemie, RWTH Aachen University, D-52074 Aachen, Germany.

AUTHOR EMAIL ADDRESS: vc@iitk.ac.in; paul.koegerler@ac.rwth-aachen.de

Details of the employed Hamiltonian for the magnetochemical analysis.

For the single-ion effects the comprehensive model Hamiltonian for a d^N or an f^N metal ion in a ligand field of a specified point symmetry in an external magnetic field B is defined as

$$\hat{H} = \underbrace{\sum_{i=1}^{N}\left[-\frac{\hbar^2}{2m_e}\nabla_i^2 + V(r_i)\right]}_{\hat{H}^{(0)}} + \underbrace{\sum_{i>j}^{N}\frac{e^2}{r_{ij}}}_{\hat{H}_{ee}} + \underbrace{\sum_{i=1}^{N}\zeta(r_i)\,\kappa\,\hat{\mathbf{l}}_i\cdot\hat{\mathbf{s}}_i}_{\hat{H}_{so}} +$$

$$\underbrace{\sum_{i=1}^{N}\sum_{k=0}^{\infty}\left\{B_0^k C_0^k(i) + \sum_{q=0}^{k}\left[B_q^k\left(C_{-q}^k(i) + (-1)^q C_q^k(i)\right)\right]\right\}}_{\hat{H}_{lf}} +$$

$$\underbrace{\sum_{i=1}^{N}\mu_B\,(\kappa\,\hat{\mathbf{l}}_i + 2\hat{\mathbf{s}}_i)\cdot B}_{\hat{H}_{mag}}$$

where $H^{(0)}$ represents the energy in the central field approximation, H_{ee} and H_{SO} account for interelectronic repulsion and spin-orbit coupling (modified by the orbital reduction factor κ), respectively. The former is taken into account by the Slater-Condon parameters F^2, F^4, F^6, the latter by the one-electron spin-orbit coupling parameter ζ.[1] These sets of interelectronic repulsion parameters as well as ζ and κ are retained constant in the least-squares fitting procedure.

H_{lf} represents the electrostatic effect of the ligands in the framework of ligand field theory on the basis of the global parameters $B^k;q$ (Wyborne pseudotensors). The spherical tensors $C^k;q$ are directly related to the spherical harmonics $C^k;q = \sqrt{;4\pi/(2k+1)}\ Y^k;q$ and the real ligand field parameters $B^k;q$ are given by $A^k;q\ \langle r^k\rangle$ where $A^k;q$ is a numerical constant describing the charge distribution in the environment of the metal ion and $\langle r^k\rangle$ is the expectation value of $\langle r^k\rangle$ for

the wave function. For f electrons the terms in the expansion with $k \leq 6$ are nonzero, whereas all terms with odd k values vanish since only configurations containing equivalent electrons are considered. The values of k and q are limited by the point group of the ligand field. If the spherically symmetric term $B_0^0 C_0^0$ is ignored, in cubic systems only spherical tensors with $k = 4$ and $k = 6$ are relevant and all $B^k;q$ are zero. In the case of a ligand field with a C_4 point group the operator with reference for the angular part of the wave function reads

$$H_{\mathrm{lf}} = B_0^2 \sum_{i=1}^{N} C_0^2(i) + B_0^4 \sum_{i=1}^{N} C_0^4(i) + B_4^4 \sum_{i=1}^{N} (C_{-4}^4(i) + C_4^4(i)) + B_0^6 \sum_{i=1}^{N} C_0^4(i) + B_4^6 \sum_{i=1}^{N} (C_{-4}^4(i) + C_4^4(i))$$

In compounds **1**–**4**, the Ln^{3+} coordination environments are approximated as elongated square-antiprismatic (see Results and Discussion): The *intraplanar* distances (d_{in}), i.e. the average distance between the four neighboring ligand donor sites in each plane, the *interplanar* distances (d_{pp}), i.e. the distance between the upper and lower planes defined by the neighboring ligand donor sites, and the skew angles (ϕ), calculated as the offset between the two square planes defined by the mean planes through the coordinating atoms are also provided in Table S6. This skew angle is very close to that expected for ideal $D_{4\mathrm{d}}$ symmetry ($\varphi = 45°$). Hence, an idealized $D_{4\mathrm{d}}$ symmetry was assumed in this case. For this symmetry, the two ligand field terms with $q = 0$ ($A^4;4 \langle r^4 \rangle$ and $A^4;6 \langle r^6 \rangle$) vanish, and H_{lf} can be simplified to

$$H_{\mathrm{lf}}^{\mathrm{cyl.}} = B_0^2 \sum_{i=1}^{N} C_0^2(i) + B_0^4 \sum_{i=1}^{N} C_0^4(i) + B_0^6 \sum_{i=1}^{N} C_0^4(i) \,.$$

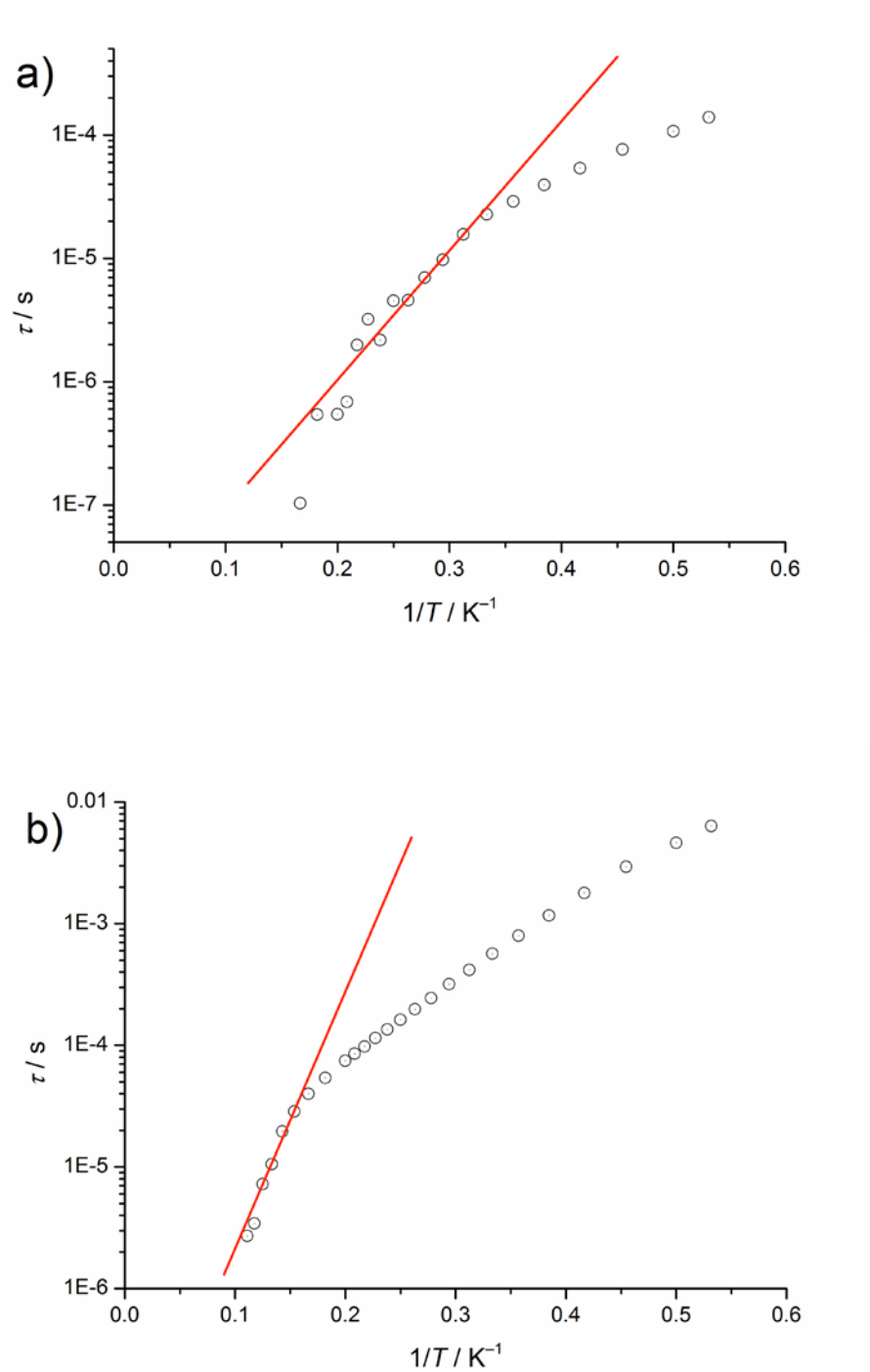

Figure S1: Linear fits to Cole-Cole equation for **1** (a) and **3** (b) producing the extrapolated time constants τ_0 and the energy barriers ΔE.

Table S1. Bond valence sum (BVS) calculations of Mn oxidation state in compounds **1-4**.

Complex	Atom	Mn^{2+}	Mn^{3+}	Mn^{4+}
1	Mn1	3.218	2.963	2.992
	Mn2	3.216	2.971	3.068
2	Mn1	3.114	2.876	2.974
	Mn2	3.208	2.965	3.065
3	Mn1	3.172	2.940	3.028
	Mn2	3.260	3.030	3.131
4	Mn1	3.215	2.971	3.071
	Mn2	3.237	3.008	3.110

Table S2. Bond valence sum (BVS) calculations for O atoms of the $[LH]^{2-}$ in complex **1**

Atom	BVS	Assignment
O4	1.102	ROH
O3	1.934	RO^-
O9	2.018	RO^-
O10	1.269	ROH
O14	1.209	ROH
O13	1.943	RO^-
O19	1.929	RO^-
O20	1.080	ROH

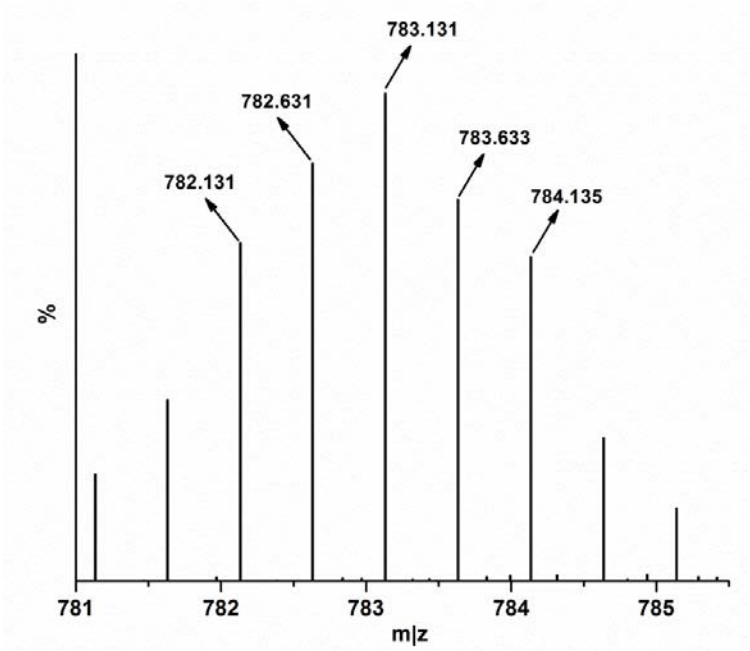

Experimental pattern

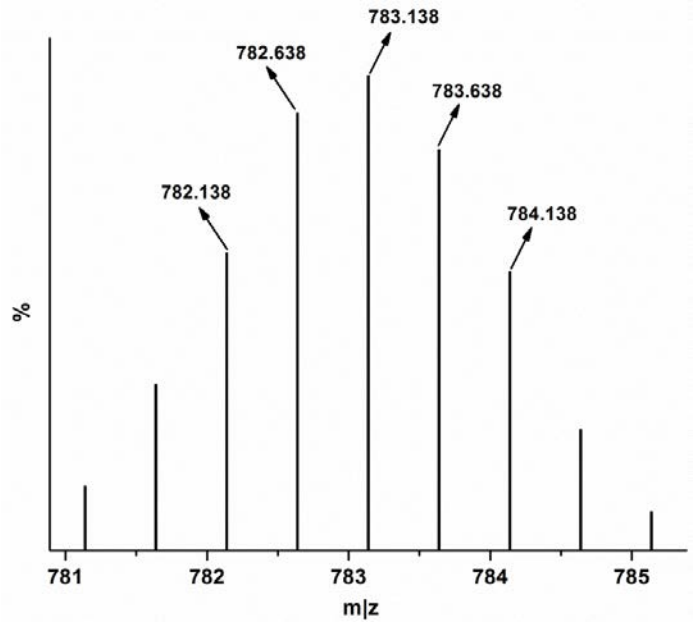

Simulated pattern

Figure S2. ESI-MS of **1**

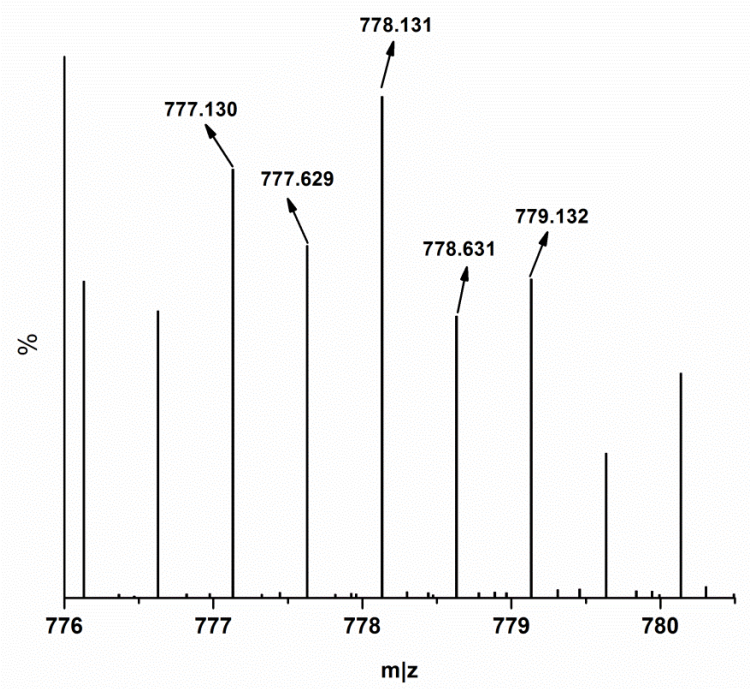

Experimental pattern

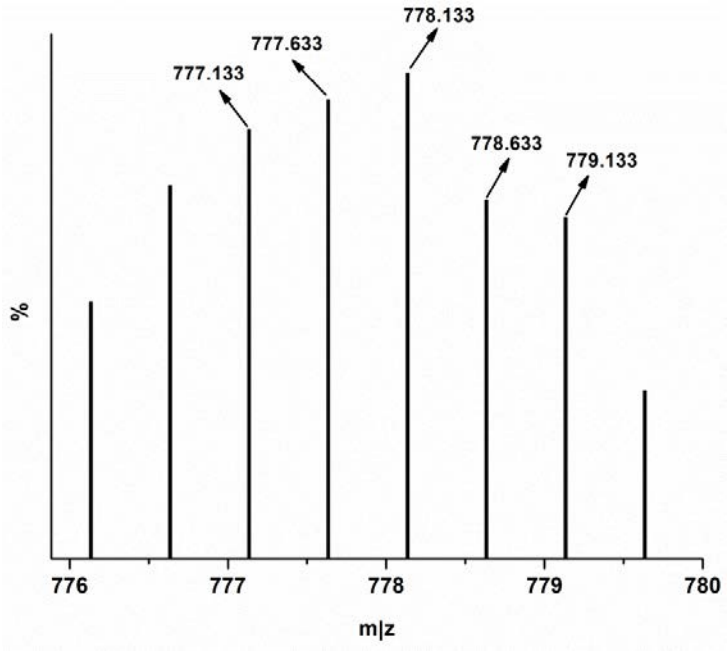

Simulated pattern

Figure S3. ESI-MS of **2**

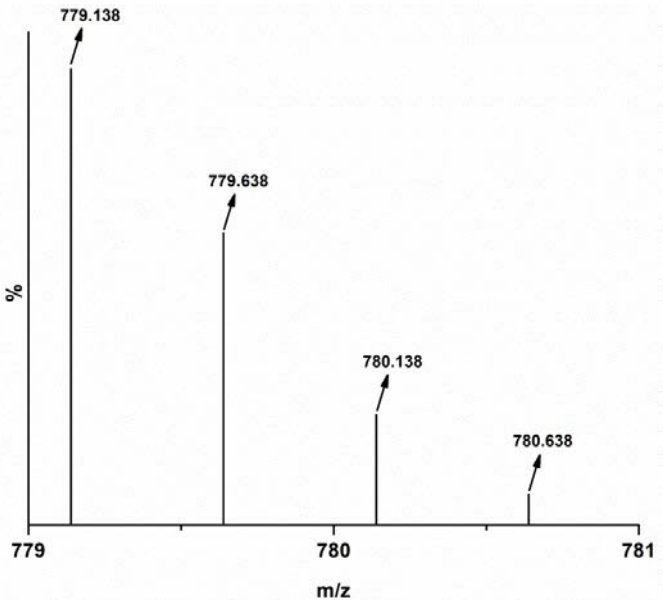

Simulated pattern

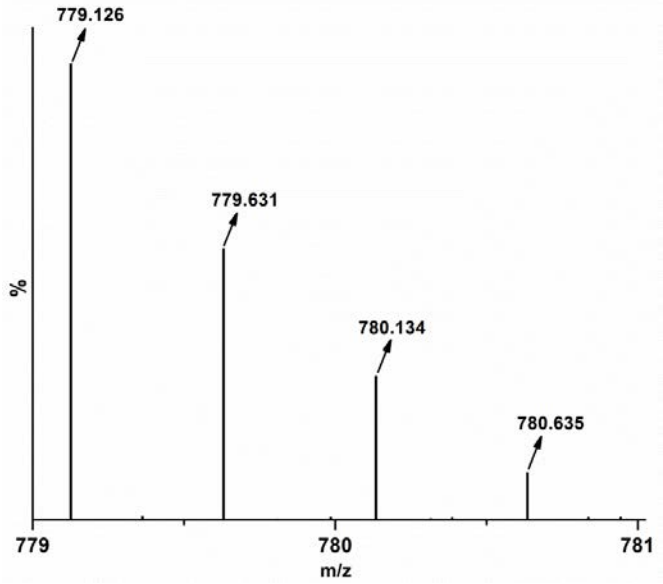

Experimental pattern

Figure S4. ESI-MS of **3**

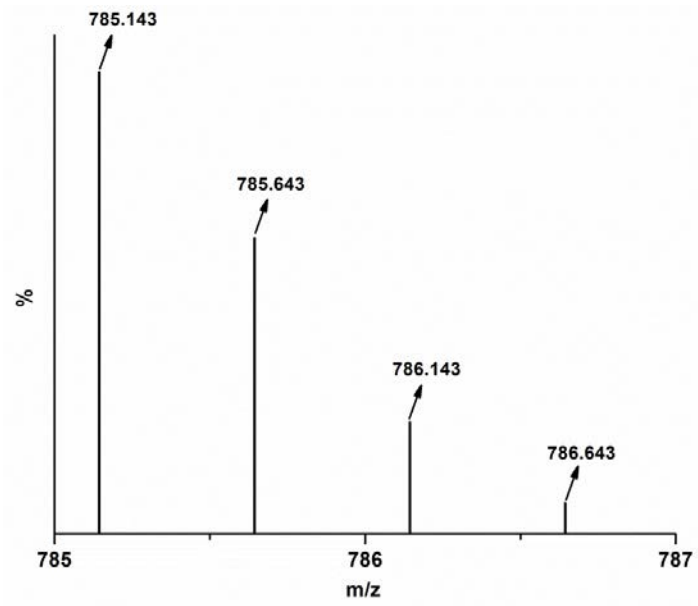

Simulated pattern

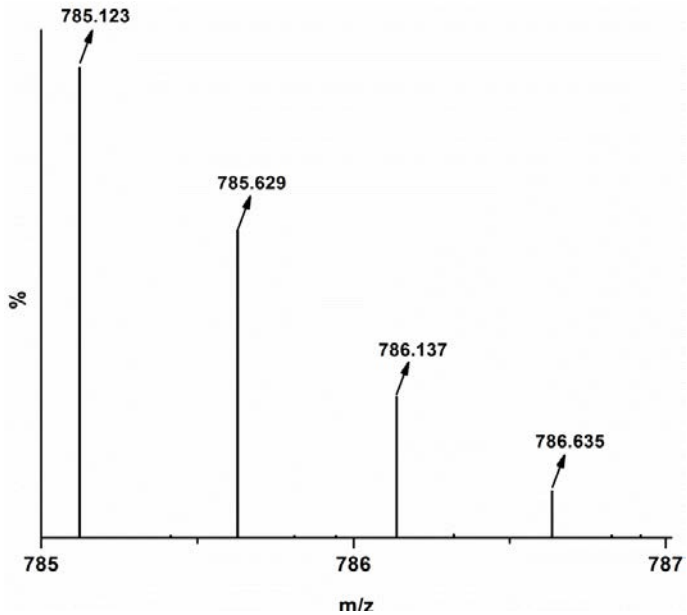

Experimental pattern

Figure S5. ESI-MS of **4**

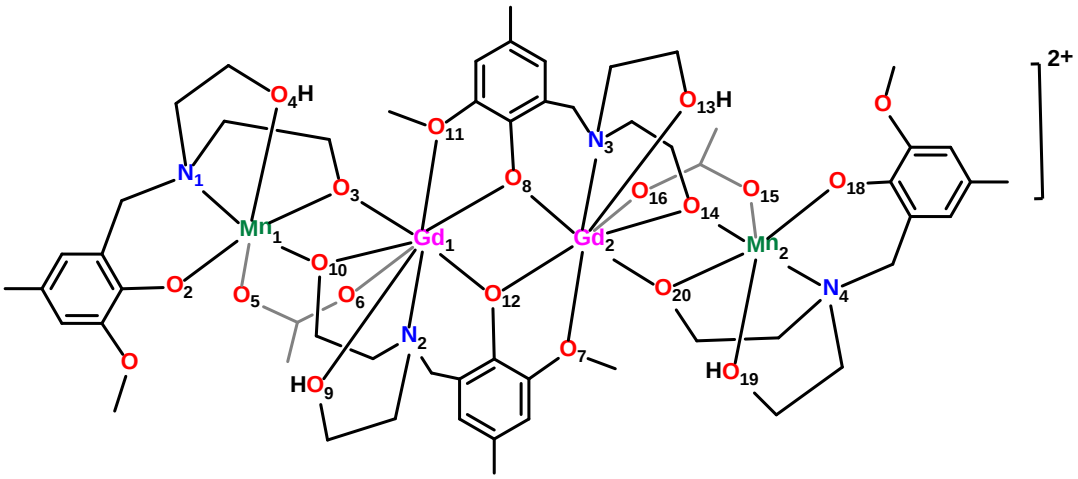

Table S3. Selected bond distances and bond angles for compound **2**

Bond lengths (Å)				Bond angles (°)	
Bond Lengths around Manganese(1)		Bond Lengths around Manganese(2)			
Mn(1)-N(1)	2.078(11)	Mn(2)-N(4)	2.062(7)	Mn(1)-O(3)-Gd(1)	101.3(2)
Mn(1)-O(2)	1.884(10)	Mn(2)-O(18)	1.865(6)	Mn(1)-O(10)-Gd(1)	101.6(3)
Mn(1)-O(3)	1.900(9)	Mn(2)-O(20)	1.907(6)	Mn(2)-O(20)-Gd(2)	101.1(2)
Mn(1)-O(13)	1.937(9)	Mn(2)-O(14)	1.916(7)	Mn(2)-O(14)-Gd(2)	102.7(3)
Mn(1)-O(5)	2.205(10)	Mn(2)-O(16)	2.203(7)	Gd(2)-O(12)-Gd(1)	106.6(2)
Mn(1)-O(4)	2.318(11)	Mn(2)-O(19)	2.305(6)	Gd(1)-O(8)-Gd(2)	106.4(2)
				Mn(1)-Gd(1)-Gd(2)	133.79(12)
Bond Lengths around Gadolinium(1)		Bond Lengths around Gadolinium(2)		Mn(2)-Gd(2)-Gd(1)	133.66(2)
Gd(1)-O(6)	2.320(6)	Gd(2)-O(15)	2.308(7)		
Gd(1)-O(10)	2.325(6)	Gd(2)-O(14)	2.325(6)		
Gd(1)-O(8)	2.328(6)	Gd(2)-O(12)	2.329(6)		
Gd(1)-O(12)	2.344(6)	Gd(2)-O(8)	2.352(6)		
Gd(1)-O(3)	2.357(6)	Gd(2)-O(20)	2.378(6)		
Gd(1)-O(9)	2.412(6)	Gd(2)-O(13)	2.399(7)		
Gd(1)-O(11)	2.494(6)	Gd(2)-O(7)	2.508(6)		
Gd(1)-N(3)	2.625(7)	Gd(2)-N(2)	2.618(8)		

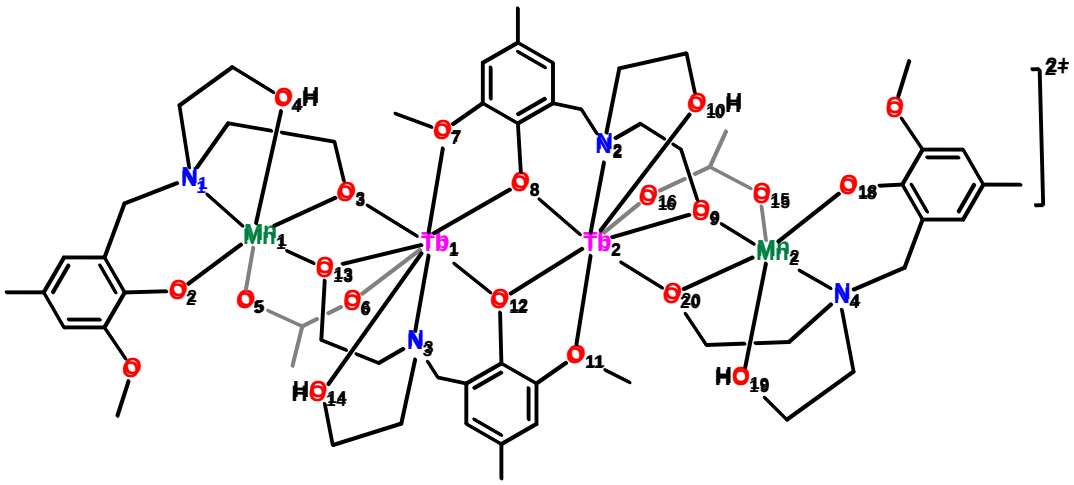

Table S4. Selected bond distances and bond angles for compound **3**

Bond lengths (Å)				Bond angles (°)	
Bond Lengths around Manganese(1)		Bond Lengths around Manganese(2)			
Mn(1)-N(1)	2.082(7)	Mn(2)-N(4)	2.056(11)	Mn(1)-O(3)-Tb(1)	101.3(4)
Mn(1)-O(2)	1.863(6)	Mn(2)-O(18)	1.850(9)	Mn(1)-O(13)-Tb(1)	101.5(4)
Mn(1)-O(3)	1.902(6)	Mn(2)-O(20)	1.899(8)	Mn(2)-O(9)-Tb(2)	102.7(4)
Mn(1)-O(10)	1.931(6)	Mn(2)-O(9)	1.902(10)	Mn(2)-O(20)-Tb(2)	101.3(4)
Mn(1)-O(5)	2.207(7)	Mn(2)-O(15)	2.211(10)	Tb(2)-O(8)-Tb(1)	106.6(3)
Mn(1)-O(4)	2.293(7)	Mn(2)-O(19)	2.310(12)	Tb(1)-O(12)-Tb(2)	105.7(3)
				Mn(1)-Tb(1)-Tb(2)	133.85(4)
Bond Lengths around Terbium(1)		Bond Lengths around Terbium(2)		Mn(2)-Tb(2)-Tb(1)	133.81(4)
Tb(1)-O(6)	2.304(9)	Tb(2)-O(16)	2.303(9)		
Tb(1)-O(13)	2.313(9)	Tb(2)-O(8)	2.318(8)		
Tb(1)-O(12)	2.314(8)	Tb(2)-O(9)	2.322(9)		
Tb(1)-O(8)	2.321(9)	Tb(2)-O(12)	2.351(8)		
Tb(1)-O(14)	2.352(9)	Tb(2)-O(20)	2.361(8)		
Tb(1)-O(3)	2.352(9)	Tb(2)-O(10)	2.371(11)		
Tb(1)-O(7)	2.482(8)	Tb(2)-O(11)	2.502(9)		
Tb(1)-N(3)	2.633(11)	Tb(2)-N(2)	2.608(11)		

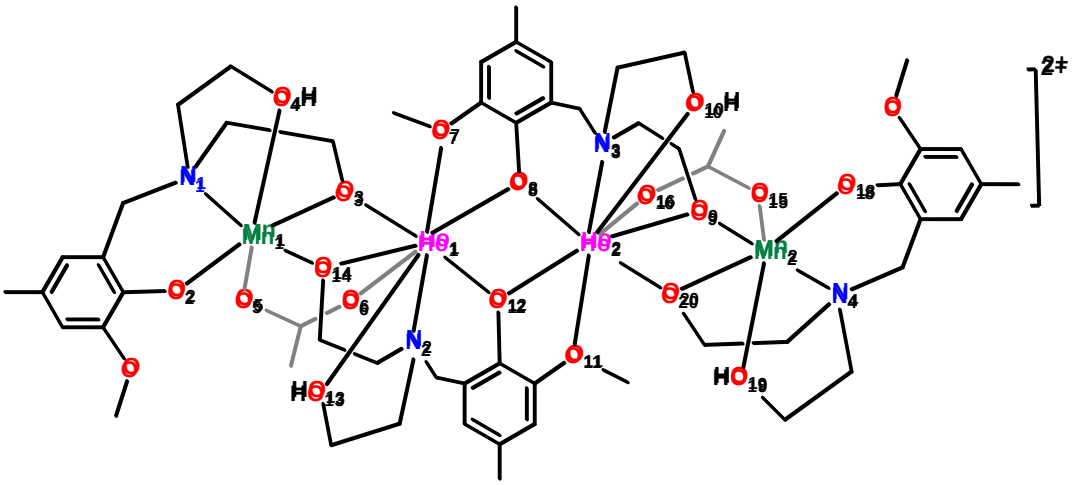

Table S5. Selected bond distances and bond angles for compound **4**

Bond lengths (Å)				Bond angles (°)	
Bond Lengths around Manganese(1)		Bond Lengths around Manganese(2)			
Mn(1)-N(1)	2.069(17)	Mn(2)-N(4)	2.059(16)	Mn(1)-O(3)-Ho(1)	101.8(6)
Mn(1)-O(2)	1.857(13)	Mn(2)-O(18)	1.853(13)	Mn(1)-O(14)-Ho(1)	102.8(6)
Mn(1)-O(3)	1.879(13)	Mn(2)-O(9)	1.899(13)	Mn(2)-O(9)-Ho(2)	102.8(5)
Mn(1)-O(14)	1.912(14)	Mn(2)-O(20)	1.905(13)	Mn(2)-O(20)-Ho(2)	100.5(5)
Mn(1)-O(5)	2.200(14)	Mn(2)-O(16)	2.239(14)	Ho(1)-O(8)-Ho(2)	106.5(5)
Mn(1)-O(4)	2.422(15)	Mn(2)-O(19)	2.287(15)	Ho(1)-O(12)-Ho(2)	106.2(5)
Bond Lengths around Holmium(1)		Bond Lengths around Holmium(2)		Mn(1)-Ho(1)-Ho(2)	133.59(6)
Ho(1)-O(6)	2.294(14)	Ho(2)-O(15)	2.283(14)	Mn(2)-Ho(2)-Ho(1)	134.44(6)
Ho(1)-O(8)	2.295(12)	Ho(2)-O(9)	2.298(13)		
Ho(1)-O(12)	2.295(13)	Ho(2)-O(8)	2.308(12)		
Ho(1)-O(14)	2.300(13)	Ho(2)-O(12)	2.315(13)		
Ho(1)-O(3)	2.356(13)	Ho(2)-O(10)	2.356(14)		
Ho(1)-O(13)	2.365(14)	Ho(2)-O(20)	2.357(12)		
Ho(1)-O(7)	2.467(13)	Ho(2)-O(11)	2.469(14)		
Ho(1)-N(2)	2.587(16)	Ho(2)-N(3)	2.556(17)		

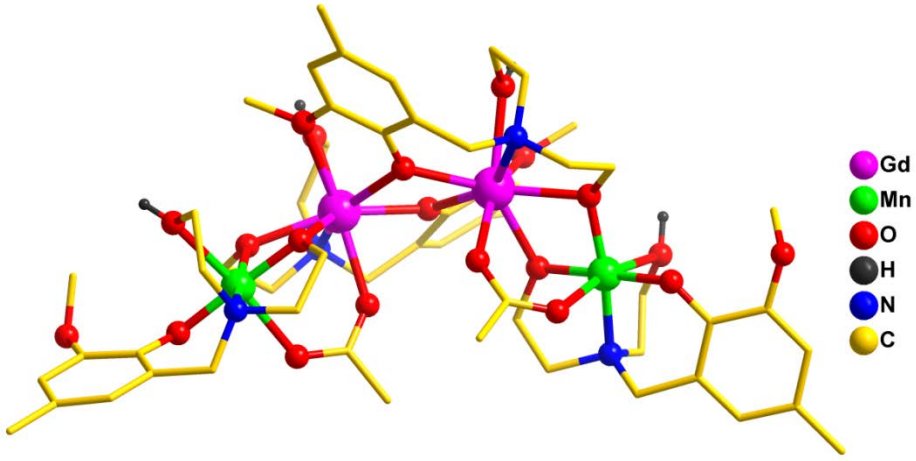

Figure S6. Molecular structure of **2**, hydrogen atoms, counter anions and solvent molecules were omitted for clarity.

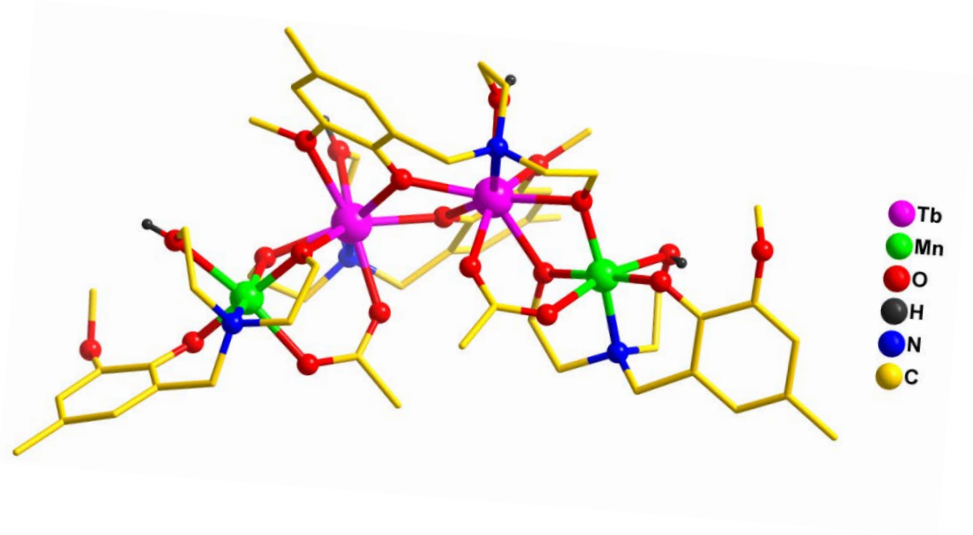

Figure S7. Molecular structure of **3**, hydrogen atoms, counter anions and solvent molecules were omitted for clarity.

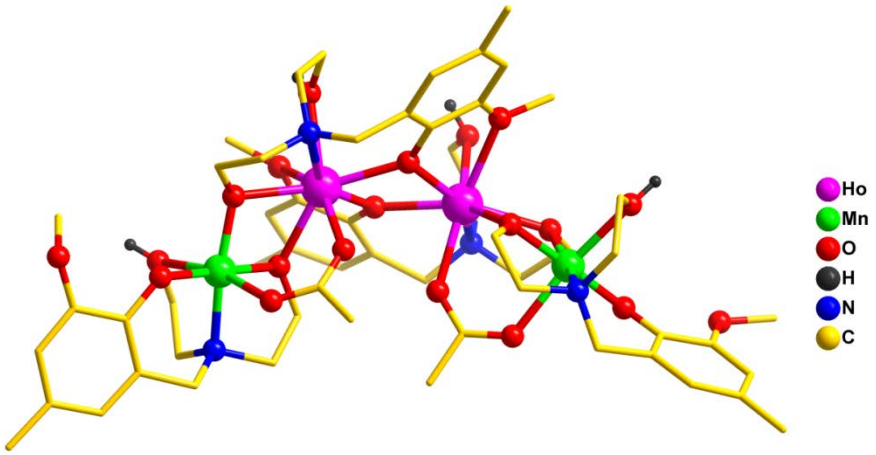

Figure S8. Molecular structure of **4**, hydrogen atoms, counter anions and solvent molecules were omitted for clarity.

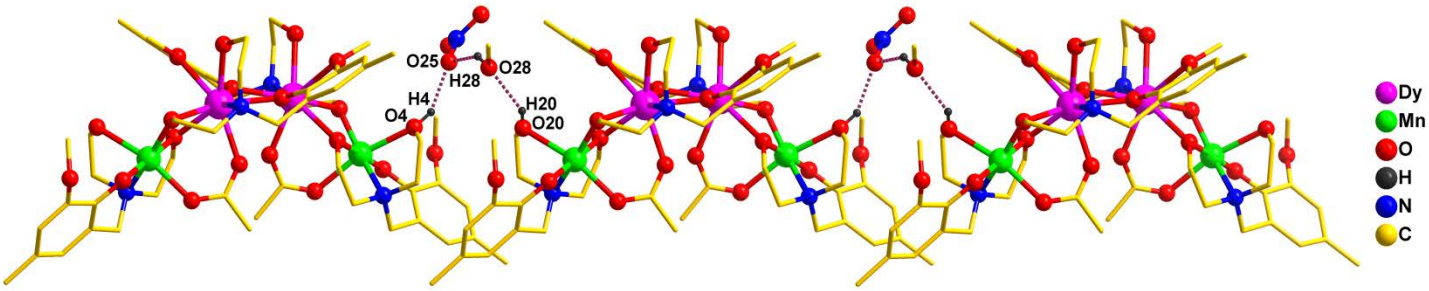

Figure S9: Formation of one dimensional chain through O–H….O interactions in **1** mediated by nitrate counter anion.

Table S6: Hydrogen bond parameters for compound **1**

Compounds	D–H….A	d(D–H)	d(H….A)	d(D….A)	<(DHA)	Symmetry of A
1	O4–H4….O25	0.858(14)	1.929(13)	2.675(18)	144.62(11)	x, 1+y, z
	O28– H28….O25	0.821(22)	1.879(19)	2.590(31)	144.17(15)	x, 1+y, z
	O20– H20….O28	0.682(12)	2.054(12)	2.646(15)	145.63 (15)	x, 1+y, z

Abbreviation: D = Hydrogen bond donor, A = Hydrogen bond acceptor

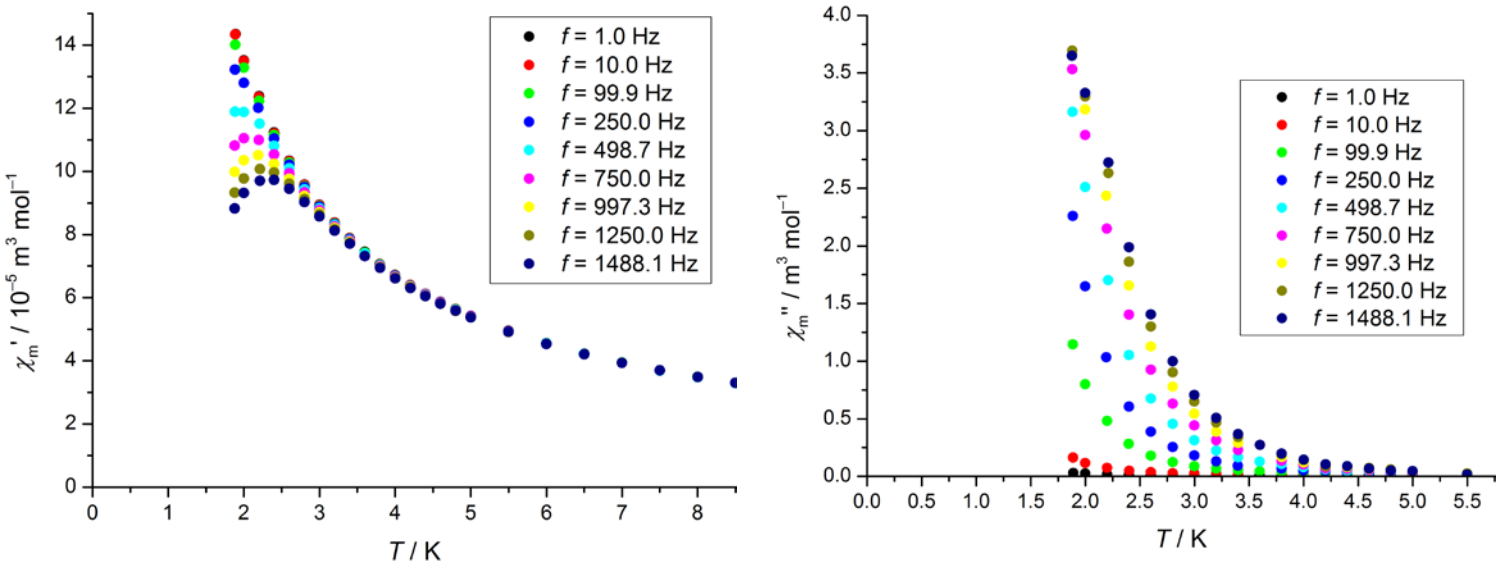

Figure S10. Temperature dependence of the in-phase χ' (left) and out-of-phase χ'' (right) ac susceptibility signals under zero dc field for **1**.

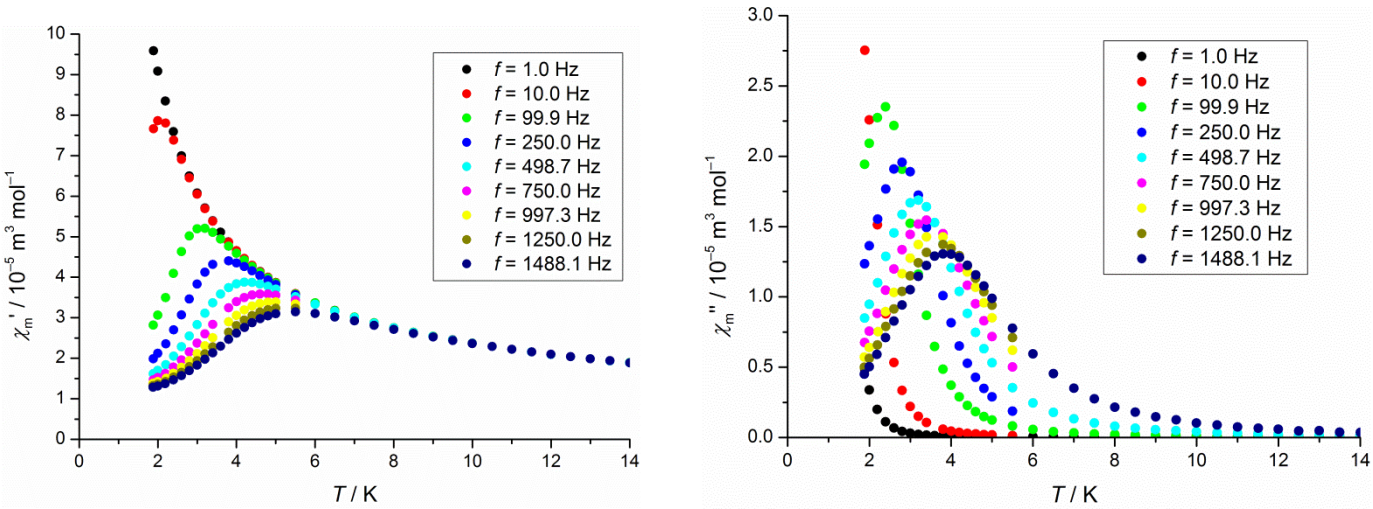

Figure S11. Temperature dependence of the in-phase χ' (left) and out-of-phase χ'' (right) ac susceptibility signals under zero dc field for **3**.

Table S7. Calculation of skew angle (ϕ), intra-planar distance (d_{ip}) and inter-planar distance (d_{pp}) to determine the geometry around lanthanide(III) ions

Compound	skew angle (ϕ)[a] (°)	Intra-planar distance (d_{ip}) (Å)	Inter-planar distance (d_{pp}) (Å)
1	46.571	2.782	2.654
2	46.448	2.841	2.685
3	46.398	2.787	2.675
4	46.447	2.771	2.650

(a) ϕ has been determined taking the average over all four dihedral angles around the lanthanide(III) ions

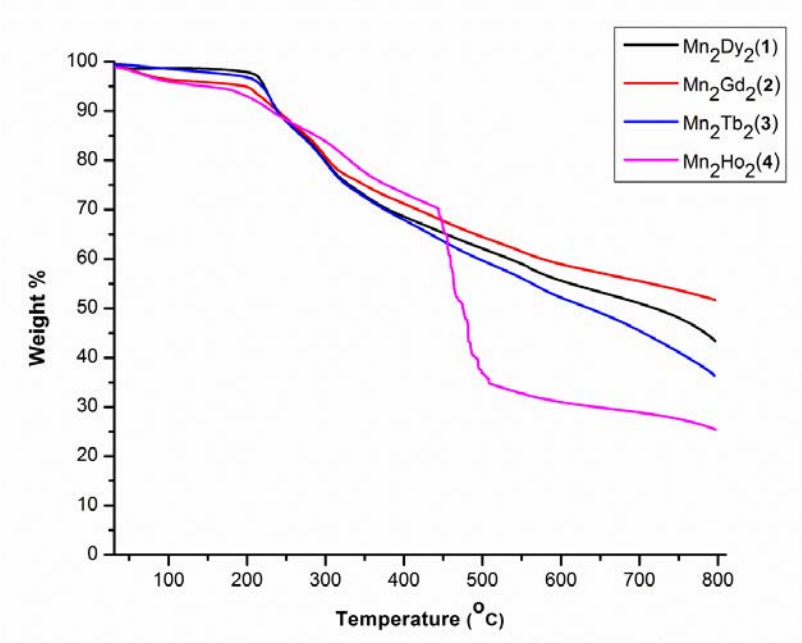

Figure S12. Thermogravimetric analysis curves of compounds **1–4** (heating rate: 10 K min^{-1}).

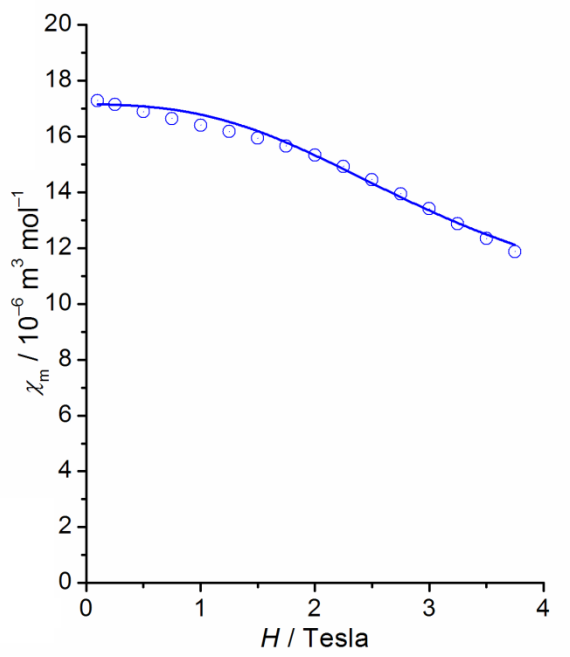

Figure S13. Field dependence of χ_{mol} for compound **2** at 2.0 K. Open circles: experimental data, solid graph: best fit to model Hamiltonian (see Table 3 for parameters).

Reference.

1 Tanner, P. A.; Kumar, V. V. R. K.; Jayasankar, C. K.; Reid, M. F. *J. Alloys Compd.* **1994**, *215*, 349.